Journal of Magnetics 17(2), 115-123 (2012) http://dx.doi.org/10.4283/JMAG.2012.17.2.115

Performance Analysis of Contactless Electrical Power Transfer for Maglev

S. Hasanzadeh and S. Vaez-Zadeh*

School of Electrical and Computer Engineering, Faculty of Engineering, University of Tehran
North Kargar Ave., P.O. Box: 14395/515, Tehran, Iran

(Received 8 March 2012, Received in final form 15 April 2012, Accepted 16 April 2012)

Contactless electrical power transfer through an air gap is a revived technology for supplying energy to many movable applications including Maglev. In this paper, magnetic equivalent circuits and analytical models of contactless electrical power transfer systems are developed and evaluated through experiment. Overall coupling coefficient and overall efficiency are introduced as means for evaluating the systems' performance. Compensating capacitors in primary and secondary sides of the systems improve the overall coupling coefficient and overall efficiency. Using the analytical models, the effects of different parameters and variables such as air gap and load current are analyzed to give a high coupling coefficient and an improved efficiency of power transfer for different compensation structures.

Keywords : contactless electrical power transfer, inductive power transfer, efficiency, resonant capacitors, maglev

1. Introduction

In some Maglev systems the required energy for support and guidance magnets and other auxiliary power systems is provided by linear generators where the maximum energy is proportional to the velocity of the vehicle [1]. However, linear generators cannot provide sufficient power for Maglev at lower speeds. Therefore, the power supply realized by conventional technology i.e. collector-feeder power rail suffers from problems such as wear and tear, noise and sparks as well as requiring the use of a contacted breaking system [2]. Another method is to add a high frequency current to the original current of the long stator of the linear drive motor to provide power to the Maglev [3].

Recently, contactless electrical power transfer (CEPT) systems have been widely investigated. This modern technique creates new possibilities in supplying movable devices with electrical energy without wires, cables, connectors and/or slip-rings which improves reliability and provides maintenance-free operation in critical applications, such as Maglev, aerospace, robotics and biomedical systems [4, 5].

Maglev systems with linear synchronous motors use the long stator concept with motor winding being part of the guide way that provides the propulsion energy. The primary windings are distributed along the track resulting in substantial increases in the construction and maintenance costs. Placing windings on the mover in conjunction with a CEPT system considerably reduces these costs. Therefore, a suitable structure should be designed to provide the best system performance. The simplicity of implementation, taking into account the practical limitations, is essential when selecting the CEPT structure.

CEPT can be achieved by different methods; among them the inductive power transfer (IPT) method enjoys advantages such as lack of erosion, high reliability, insensitivity to environmental conditions, pollution free operation and requires little maintenance or control tools [5]. Different applications of CEPT range from the charging of low power home and office instruments to high power transportation and industrial applications such as cranes, ground floor transportation systems, monorails, vehicles, elevators and battery charging systems. Nevertheless, CEPT theory and technology are far from maturity and suffer from difficulties such as weak coupling coefficients and low efficiency.

The modeling of CEPT systems has been considered but no calculations of efficiency or coupling coefficient (CC) were presented [6]. Equivalent magnetic circuits of CEPT systems have been employed to calculate, analyze and compare the coupling coefficient, efficiency and other

*Corresponding author: Tel: +9861114361
Fax: +98 (21) 88778690/88633029,
e-mail: vaezs@ut.ac.ir

characteristics of two CEPT structures [7, 8]. However, the improvement of the CC and efficiency of the systems was not considered. On the other hand, several pieces of research looked into the improvement of weak CC and efficiency of CEPT systems by using compensation circuits. An optimization was carried out for the selection of economical and efficient CEPT system structures and their resonant capacitors [9]. A resonant circuit has also been proposed for inclusion in the primary side of CEPTs [10]. An optimal operating frequency range regarding high efficiency operation of a CEPT has been presented [11]. However, previous works do not investigate generally the coupling coefficient and efficiency of the compensated systems. Also, a comparison of the CC and the efficiency of the compensated and uncompensated CEPT systems have not been reported.

This paper aims to perform a thorough analysis of capacitor-compensated CEPT systems that meet resonance conditions. New concepts of overall coupling coefficient (OCC) and overall efficiency (OE) are introduced to accommodate the assessment of the compensated systems' performance. Using these concepts, a comparison is made between the CC and the efficiency of the compensated and uncompensated systems with varying air gaps and the gain achieved by the resonant circuits is investigated quantitatively. A CEPT system is simulated for a typical Maglev system. Then, the experimental setup is implemented to verify the results obtained by analytical simulations. Overall coupling coefficient and overall efficiency of the compensated system are proved to be much higher than the coupling coefficients and efficiency of the uncompensated system, respectively.

2. System Description

In contactless operation, the power transfer apparatus is very similar to a transformer, except in this case the core material is split into two halves and the two sides do not touch, but are separated by a small air gap. This split core arrangement provides the inductive power transfer. The primary side operates as a primary inductor and is located on the stationary base unit. The secondary side is located on the vehicle and operates as a pickup inductor. The pickup inductor effectively receives the power transmitted by the primary inductor and delivers it as AC power to the vehicle. The power can be used immediately by the traction motor or can be stored for later use. The electrified primary inductor together with the pick-up inductor could be shared with levitation magnets.

Fig. 1 shows an arrangement of the contactless power transfer units for a Maglev train and a cross section of the inductors where the pickup inductor is suspended within 10-50 mm of the guideway track. The track is segmented. Each segment is energized only when the train approaches. Each segment of the primary inductor is typically up to a hundred meter long. The pickup inductor mounted on the vehicle is about 2-5 meter long, depending on the vehicle's size and energy requirements. The pickup inductor is much shorter than the primary inductor. Therefore, the total energy loss in the pickup inductor is generally less than that in the primary one even though the pickup inductor operates at much higher flux levels than the primary inductor. The turn number of the pickup inductor is set in accordance with the required power.

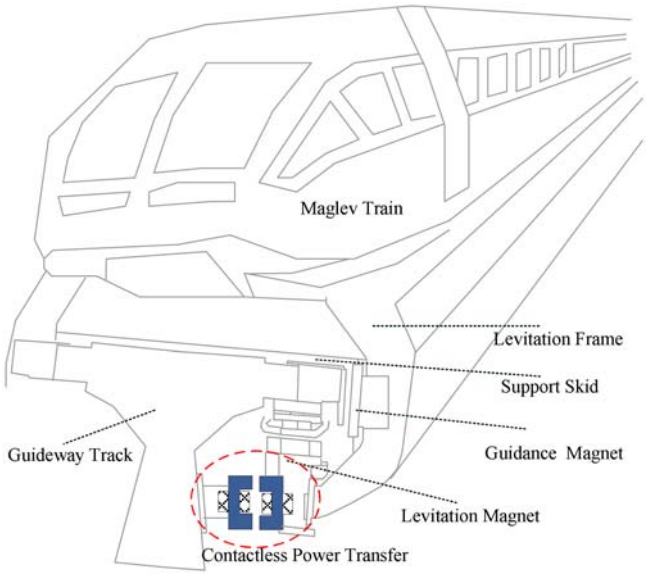

Fig. 1. (Color online) Cross section of the CEPT system for a Maglev.

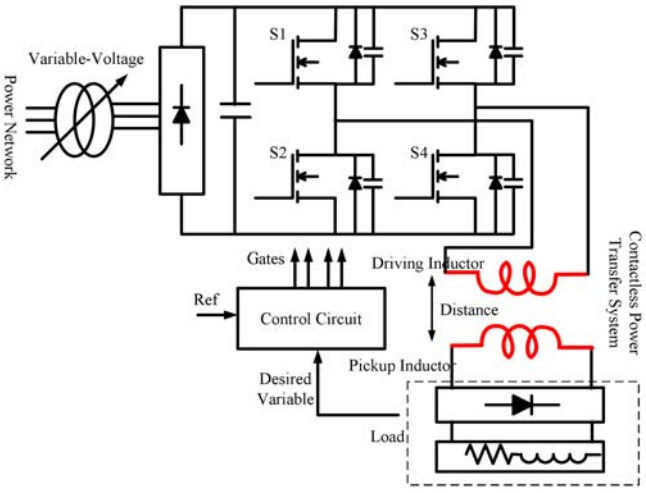

Fig. 2. (Color online) Fundamental Schematic of the CEPT-System.

To the enhance CEPT system efficiency, each segment of the track is supplied by a high frequency power supply. Fig. 2 shows a full-bridge inverter topology, converting a single or a three phase input power to a high frequency output power. The high frequency power is delivered to the pickup inductor through a magnetic field. The size and cost of all components of the CEPT system can be reduced by increasing the frequency. It is an appropriate to set the frequency in the range of 10 kHz to 30 kHz to achieve a high power rating [2].

The power circuit on the pickup side consists of a switchable ac capacitor bank, a rectifier, several inductors, and a dc filter. There are also sensors and a control system. The ac capacitors perform as part of a resonant circuit. Generally, increasing the capacitance increases the output current.

3. System Model

In this work, a contactless inductive power transfer system is investigated. The equivalent circuit to a transformer is used as the first step to model the system. This circuit is usually described by a magnetizing inductance and two leakage inductances, where the former is much higher. As such, the leakage inductances can be ignored. However, in contactless systems, the leakage inductances are very large and cannot be ignored. Thus, an electromagnetic system with weak coupling should be described by modeling the leakage inductances, magnetizing inductance and mutual inductance.

3.1. Electrical Circuit Model

Here, the contactless power transfer system is modeled as a transformer with the mutual inductance of a weak electromagnetic coupling. The model variables and parameters are the primary circuit voltage V_s, impedances of the primary and pickup circuits Z_1 and Z_2, the primary and pickup inductances and resistances L_1, L_2 and R_1, R_2 and the mutual inductance M. A large leakage inductance (sometimes larger than the magnetizing inductance) increases the power loss and hence reduces the transfer efficiency. For this reason, resonant capacitors must be utilized in CEPT circuits. Fig. 3 shows different structures in which the series and parallel resonant capacitors for the primary and pickup sides have been inserted. Four different structures can be formed with these resonant capacitors: series-series (SS), series-parallel (SP), parallel-series (PS) and parallel-parallel (PP) connections.

According to Fig. 3, model of inductive power transfer can be stated by:

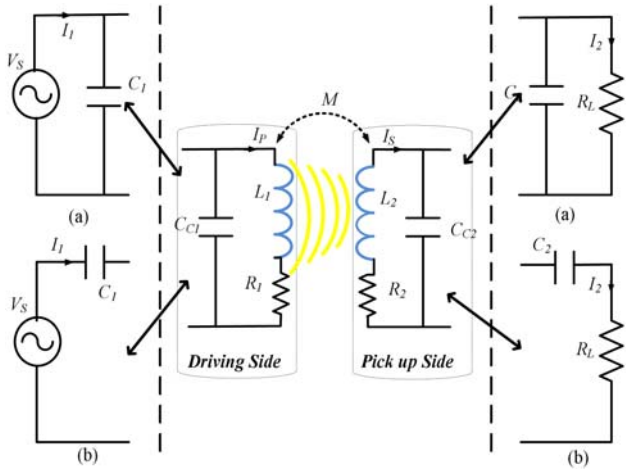

Fig. 3. (Color online) Circuit model of the system with resonant capacitors, (a) P (Parallel) and (b) S (Series) capacitor connection on both sides.

$$V_s = Z_1 I_1 - j\omega M I_2$$
$$0 = -j\omega M I_1 + Z_2 I_2 \tag{1}$$

where Z_1 and Z_2 are the primary and pickup impedances of the system without coupling, respectively. These impedances are found, for the SS structure by:

$$Z_1 = R_1 + j\left(L_1\omega - \frac{1}{C_1\omega}\right)$$
$$Z_2 = R_2 + R_L + j\left(L_1\omega - \frac{1}{C_2\omega}\right) \tag{2}$$

The efficiency of the system for SS and PS structures is obtained by:

$$\eta_S = \frac{(\omega M)^2 R_L}{Z_2(Z_1 Z_2 + (\omega M)^2)} \tag{3}$$

while the efficiency of the system for SP and PP structures is given by:

$$\eta_P = \frac{(\omega M)^2}{Z_2(Z_1 Z_2 + (\omega M)^2)} \frac{R_L}{1 + (R_L C_2 \omega)^2} \tag{4}$$

The uncompensated system efficiency according to (3) and (4) is therefore calculated as:

$$\eta = \frac{R_L}{(R_2 + R_L)\left(1 + \frac{R_1(R_2 + R_L)}{(\omega M)^2}\right) + \frac{R_1 L_2^2}{M^2}} \tag{5}$$

Also, the overall efficiency of the compensated system is given for series and parallel capacitors for the pickup side are respectively given as [9]:

$$\eta_S = \frac{R_L}{(R_L + R_2)\left(1 + R_1 \dfrac{R_2 + R_L}{(\omega_0 M)^2}\right)} \tag{6}$$

$$\eta_P = \frac{R_L}{R_L + R_2 + \dfrac{R_2 R_L^2}{(\omega_0 L_2)^2} + \dfrac{R_1 R_2^2}{(\omega_0 M)^2} + \dfrac{R_1 L_2^2}{M^2}} \tag{7}$$

3.2. Magnetic Equivalent Circuit Model

A section of the contactless power transfer system for maglev with its specifications is presented in the Appendix and depicted in Fig. 4. Here the primary and pickup inductors are located on the stationary track and movable vehicle, respectively. The magnetic equivalent circuit (MEC) of the system is also illustrated in the same figure, where the power transfer losses are due to the magnetic flux leakages (R_{l1}, $R_{l2,\ldots,}$ R_{l5}), core losses of the magnetic flux paths (R_1, $R_{2,}$ …, R_6) and losses related to the air gaps (R_{g1}, R_{g2}). The coupling coefficient, main and mutual inductances are calculated by using the MEC. The primary and the pickup inductances are given by:

$$L_1 = \frac{N_1^2}{\Re_{eq1}} \tag{8}$$

$$L_2 = \frac{N_2^2}{\Re_{eq2}} \tag{9}$$

The mutual inductance indicates the degree of magnetic coupling between the primary and pickup inductors. It measures the magnetic flux lines that link (or couple) the primary and pickup inductors. The mutual inductance is inversely proportional to the air gap length given by the relation:

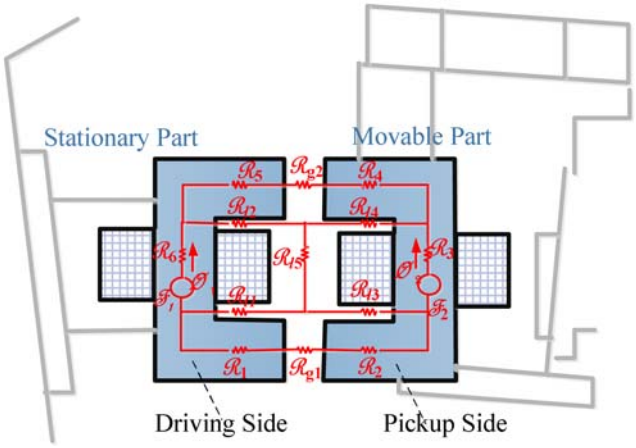

Fig. 4. (Color online) CEPT section of Maglev with its Magnetic equivalent circuit.

$$M = \frac{N_1 N_2}{\Re_{eq1}} \frac{\Re_{33}}{\Re_{22} + \Re_{33}} \tag{10}$$

where $\Re_{eq1}$ and $\Re_{eq2}$ are the equivalent reluctances from the primary and pickup sides. All variables calculated by MEC are presented in the Appendix.

$$k = \frac{M}{\sqrt{L_1 L_2}} \tag{11}$$

It is known that the system coupling coefficient, k, is the proportion of the primary flux linked with the pickup inductor. Using (11) and the equivalent circuit, k is calculated by:

$$k = \sqrt{\frac{\Re_{eq2}}{\Re_{eq1}}} \frac{\Re_{33}}{\Re_{22} + \Re_{33}} \tag{12}$$

3.3. Overall Coupling Coefficient

Considering (6) and (7) and relations of the compensated system efficiencies, we introduce a new concept; overall coupling coefficient. This allows the performance of the completely compensated systems to be investigated without using calculating the compensation capacitors.

Two overall coupling coefficients are defined for this system, taking into account that the effects of the capacitors can be calculated for series and parallel capacitors on the pickup side, respectively, by:

$$k_{ovS} = k\left(\frac{\omega_0}{\omega}\right)\sqrt{1 + \left(\frac{\omega L_2}{R_2 + R_L}\right)^2} \tag{13}$$

$$k_{ovP} = k\left(\frac{\omega_0}{\omega}\right)\sqrt{\frac{(R_2 + R_L)^2 + (\omega L_2)^2}{R_2^2 + (\omega_0 L_2)^2 + \dfrac{R_L^2 R_2 M^2}{R_1 L_2^2}}} \tag{14}$$

If it is supposed that $R_2 M^2 \cong R_1 L_2^2$ then the overall coupling coefficient for parallel capacitors on the pickup sides is obtained by:

$$k_{ovP} = k\left(\frac{\omega_0}{\omega}\right)\sqrt{1 + \frac{2R_2 R_L}{R_2^2 + R_L^2 + (\omega_0 L_2)^2}} \tag{15}$$

where $\omega_0 = 2\pi f_0$ is the angular resonant frequency .

The system performance can be evaluated with consideration of overall coupling coefficients. Suppose that, an uncompensated system with specific parameters has a coupling coefficient k and works at the operating frequency f. This system can be designed to work at the resonance frequency f_o by adjusting the corresponding coupling coefficients (overall coupling coefficient). A

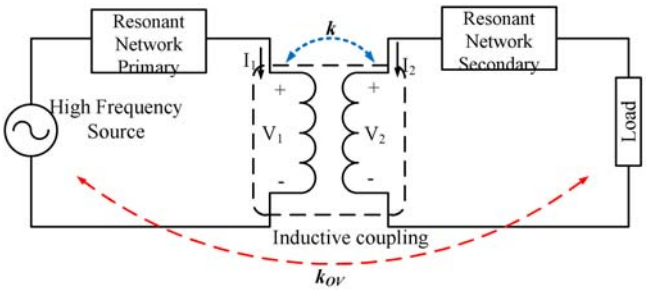

Fig. 5. (Color online) Overall coupling coefficient for the compensated system.

schematic view of the CEPT system including resonant capacitors and an introduction to the overall coupling coefficient is shown in Fig. 5.

4. Simulation Results

In this section, the set of simulation results for a CEPT system are presented for Maglev system. The primary inductor has a single turn along the primary track and the number of pick-up turns is 200. The operating frequency is 8 kHz. Using (12), the system coupling coefficient is calculated and the overall coupling coefficients are obtained from (13) and (15) as illustrated in Fig. 6. It can be seen that the overall coupling coefficients of the compensated structures are higher than those of the uncompensated structure for all air gaps.

Fig. 7 shows the system efficiency versus air gap confirming that the compensation circuit improves the system efficiency.

As shown in Figs. 6 and 7, the SS and PS structures are more efficient than the SP and PP structures for systems with an air gap smaller than 40 mm, while the SP and PP structures are more efficient for systems with an air gap

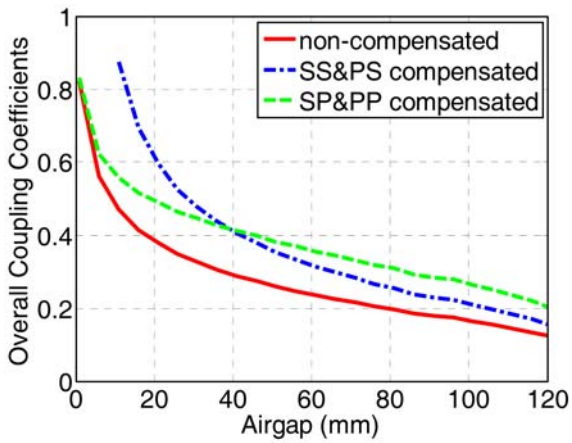

Fig. 6. (Color online) Overall coupling coefficient versus air gap.

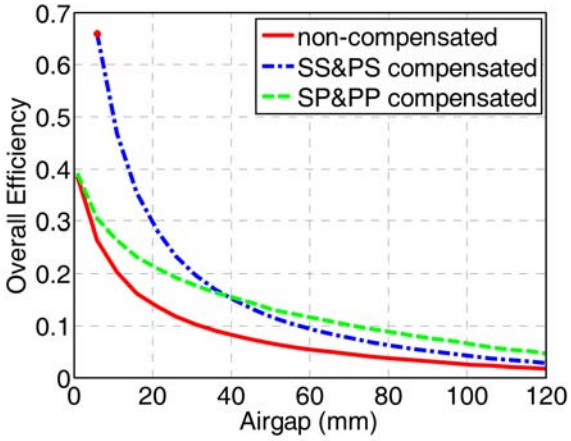

Fig. 7. (Color online) Overall efficiency versus air gap.

larger than 40 mm. According to the system parameters and operating frequency, the efficiency values for all compensated structures are the same, for an air gap of 40 mm.

Suppose that the Maglev system has a fixed velocity. Then, the required power for propulsion is constant. If the air gap is varied, the induced voltage in the pickup inductors and load power will be changed. So, the load power will vary. In order to have fixed output power for a varying air gap, a control system is required to change the supply voltage and frequency.

For large air gaps, the leakage fluxes increase and the voltage drop is high. Therefore, for fixed output voltage, the supply voltage must be increased. This voltage increase is limited in compensated systems since the required reactive current for the system is partially provided by compensated capacitors.

Figs. 8 and 9 show the supply voltage and current versus air gap respectively for a constant load current.

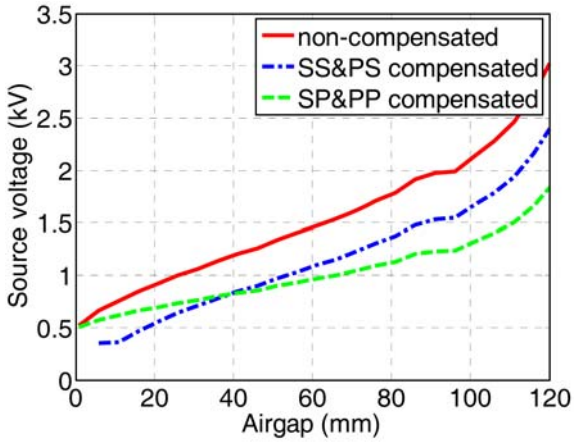

Fig. 8. (Color online) Supply voltage versus air gap at a specific load.

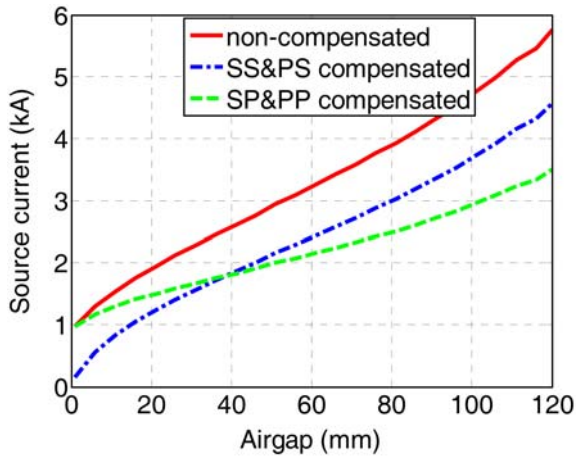

Fig. 9. (Color online) Supply current versus air gap at a specific load.

The supply current of the compensated system is less than of the uncompensated system for a specified load. Also, the supply voltage for a specified load is lower in the uncompensated system.

5. Experimental Evaluation

Since, the construction of a real size CEPT system for maglev is too costly, a scaled experimental CEPT system is built, as shown in Fig. 10. Inductor resistances (R_1, R_2) are calculated by applying a dc voltage to both CEPT system sides and measuring the current. Self-inductances are computed by (16). In the experiment, this is measured by applying an ac voltage with given frequency to the inductor and measuring its current. Mutual inductance can also be calculated by (17) where an open circuit voltage in the secondary side and a no load current in the primary side are measured. Calculated and measured self-inductances and mutual inductances are presented in Table 1.

Table 1. Determination of the System Parameters.

Air gap (mm)	Inductances L_1 and L_2 (H)	Mutual inductance M (H)
0	1.8697	1.8243
2	0.1739	0.1206
4	0.1309	0.0793
6	0.1150	0.0643
8	0.1046	0.0553
10	0.0987	0.0500
12	0.0937	0.0459
14	0.0915	0.0437
25	0.0665	0.0302

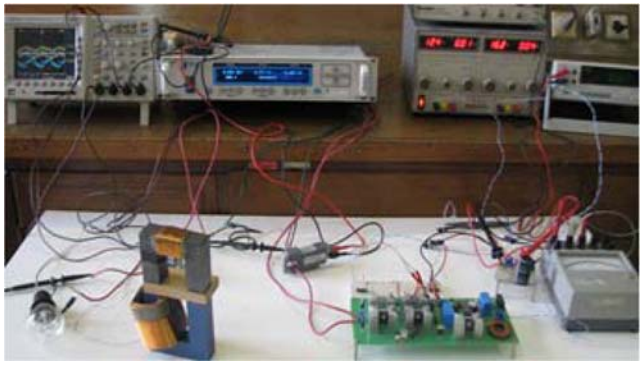

Fig. 10. (Color online) Picture of the experimental setup.

$$L_1 = \frac{1}{\omega}\sqrt{\left(\frac{V_1}{I_1}\right)^2 - R_1^2} \tag{16}$$

$$M = \frac{1}{\omega}\frac{V_{o.c2}}{I_1} \tag{17}$$

The resonance frequency is approximately equal to the product of the inductance and capacitance ($\omega_0 \cong 1/\sqrt{LC}$). In conditions where the inductance varies with the air gap, resonance conditions are provided in two ways: by the varying frequency with fixed capacitance or a fixed frequency with varying capacitance. In this work, the resonance frequency is unchanged and variable bank capacitor values are chosen for providing resonance conditions.

The system coupling coefficient versus air gap, calculated by (12) and obtained by experiment is shown in Fig. 11. It can be seen that a close agreement exists between the two sets of results.

Next, (13) and (15) are evaluated using the experimental results. The coupling coefficients for the uncompensated system and for different structures of the compensated system are depicted in Fig. 12. It can be seen

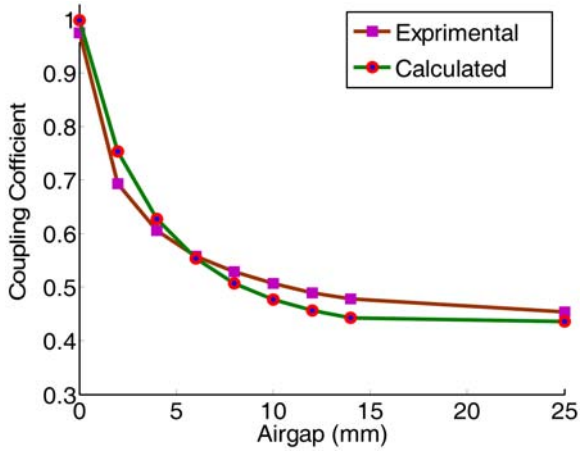

Fig. 11. (Color online) Coupling Coefficients versus air gap.

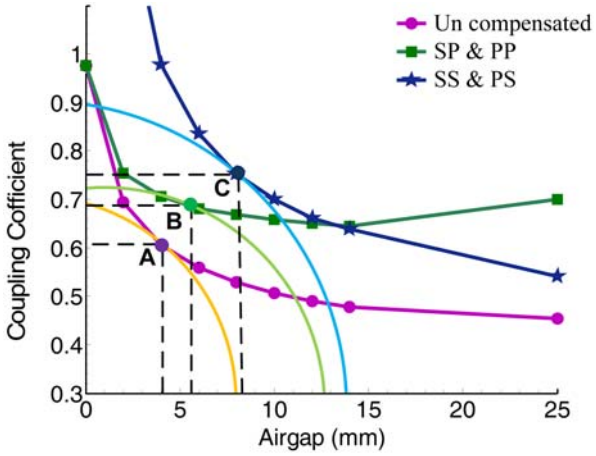

Fig. 12. (Color online) Overall coupling coefficients versus air gap.

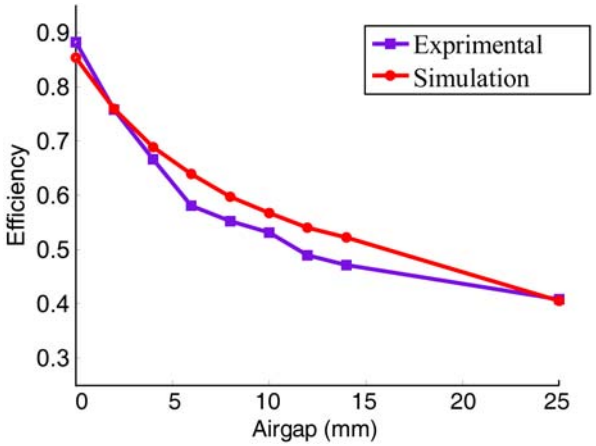

Fig. 13. (Color online) Efficiency of uncompensated structure versus air gap.

that, the uncompensated system has an optimal point, A, at which a balance between the air gap length and the coupling coefficient is achieved. However, the compensated structures provide much higher coupling factors with larger air gaps. According to Fig. 12, other optimal points, B and C, are obtained for compensated systems that have high values of overall coupling coefficient with large air gaps. It is worth mentioning that the SS and PS structures are appropriate for systems with a small air gap while the SP and PP structures are more suitable for systems with a large air gap.

The system power transfer efficiency, calculated using (13) and (15), for the non-compensated structure, obtained by experiment and simulation, is shown in Fig. 13. Experimental and simulation results of the system power transfer efficiency for compensated structures are also illustrated in Figs. 14 and 15; these show a good agreement between the simulation and experimental results. It

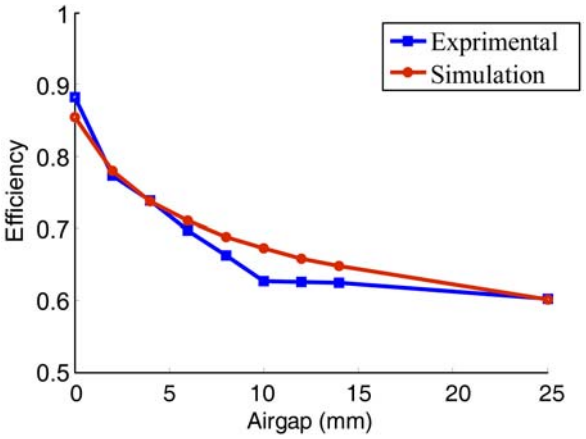

Fig. 14. (Color online) Overall efficiency of compensated structures (SP & PP) vs. air gap.

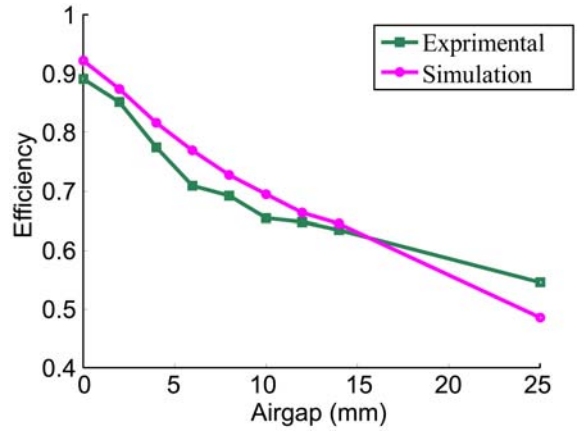

Fig. 15. (Color online) Overall efficiency of compensated structures (SS & PS) vs. air gap.

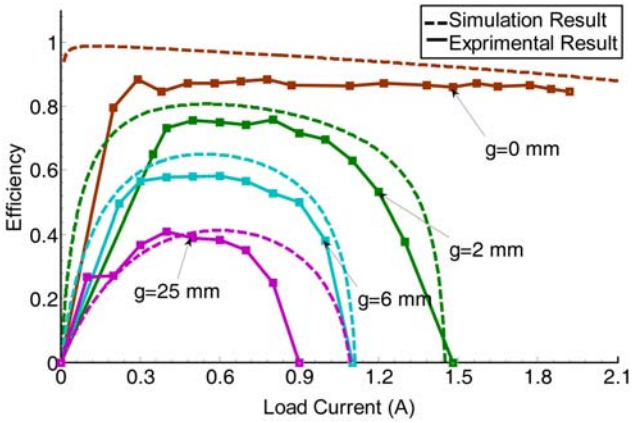

Fig. 16. (Color online) Efficiency versus load current with varying air gaps.

can also be seen that the compensated structures show a higher efficiency over a wide range of air gaps.

The effect of air gap variation on uncompensated system

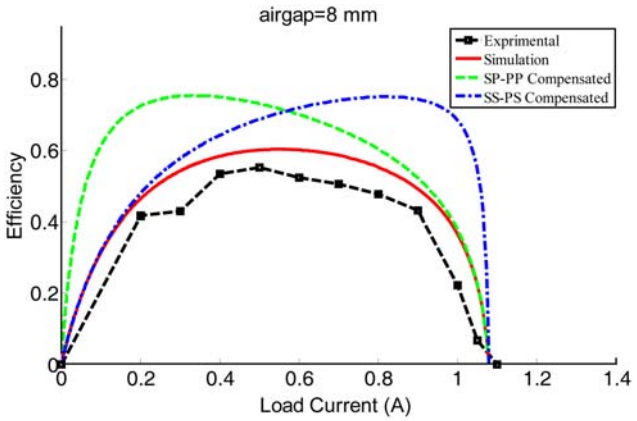

Fig. 17. (Color online) Overall efficiency of compensated structures versus load current.

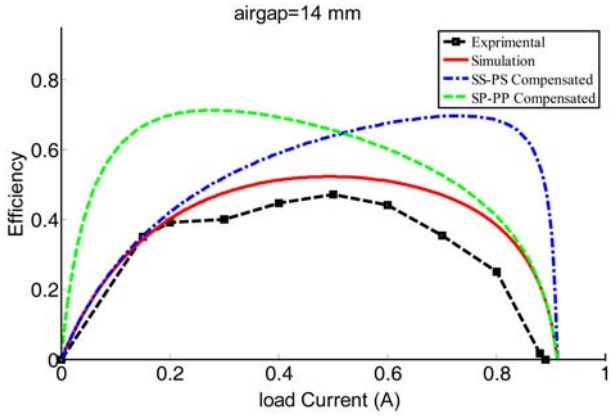

Fig. 18. (Color online) Overall efficiency of compensated structures versus load current.

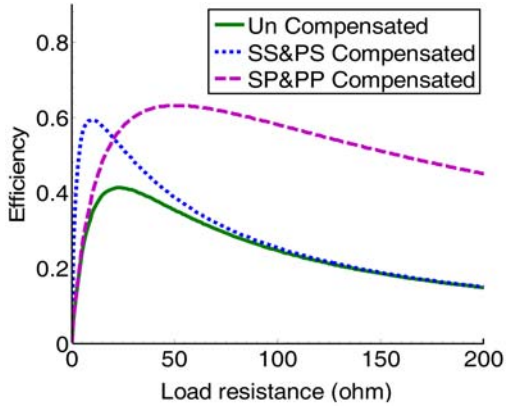

Fig. 19. (Color online) Overall efficiency of compensated structures versus load resistance.

efficiency versus load current is investigated in Fig. 16, by both simulation and experiment. It can be seen that, high efficiency in each case is achieved with a medium load range. The efficiency is reduced at high and low loads. However, the resonant circuit increases the efficiency substantially even at relative large air gaps of 8 mm and 14 mm as seen in Fig. 17 and 18, respectively. Also, the load range over which the efficiency remains at higher values is greatly extended.

Fig. 19 depicts simulation and experimental results of the overall efficiency versus load resistance for a very large air gap for all structures. It should be noted that the compensation provides improved efficiency.

6. Conclusion

An inductive contactless electrical power transfer system to supply Maglev trains was investigated using both analytical and experimental results. The system was modeled using an equivalent magnetic circuit. The overall coupling coefficient and overall efficiency of the system including the resonant circuits were then formulated. A CEPT system for supplying a Maglev train was simulated. It was shown that the overall coupling coefficients of the compensated structures are higher than those of the uncompensated structure for all air gaps. Also, the supply voltage and current required for the compensated system are less than those for the uncompensated system given a specified output power. An experimental setup was also built to evaluate the system modeling and analysis. The experimental results confirm the simulation results are accurate.

The simulation and experimental results at varying air gaps show different compensated structures of the system can improve the overall coupling coefficient and overall power transfer efficiency even at rather large air gaps. Optimal conditions are obtained for the compensated structures where a high overall coupling coefficient is obtained with large air gaps. It is worth mentioning that the SS and PS structures are more appropriate for systems with a small air gap, while SP and PP structures are more suitable for systems with large air gaps. The efficiency profile versus load current is almost constant in the compensated systems. It was also shown that the efficiency profile versus large air gaps is almost constant in the compensated system. Simulation results show that a control system must be designed to provide the proper frequency and voltage at varying air gaps for a fixed output power.

Appendix

System Specifications:

Rated load resistance	30 Ω
Primary inductor resistance	2.5 Ω
Primary inductor inductance without core	10.5 mH

Pickup inductor resistance	2.5 Ω
Pickup inductor inductance without core	10.5 mH
Operating frequency	300 Hz
Core dimensions	$102\times105\times3^2$ mm
Core material (ferrite):	
Relative permeability (μ_r)	4000
Maximum flux density (B_m)	0.35 T

Magnetic equivalent circuit parameters calculation:

$$\Re_{11} = \Re_6 + \frac{\Re_{12}(\Re_5 + \Re_{g2} + \Re_4)}{\Re_{12} + \Re_5 + \Re_{g2} + \Re_4 + \Re_{14}} + \frac{\Re_{11}(\Re_1 + \Re_{g1} + \Re_2)}{\Re_{11} + \Re_1 + \Re_{g1} + \Re_2 + \Re_{13}}$$

$$\Re_{33} = \Re_{15} + \frac{\Re_{12}\Re_{14}}{\Re_{12} + \Re_5 + \Re_{g2} + \Re_4 + \Re_{14}} + \frac{\Re_{11}\Re_{13}}{\Re_{11} + \Re_1 + \Re_{g1} + \Re_2 + \Re_{13}}$$

$$\Re_{22} = \Re_3 + \frac{\Re_{14}(\Re_5 + \Re_{g2} + \Re_4)}{\Re_{12} + \Re_5 + \Re_{g2} + \Re_4 + \Re_{14}} + \frac{\Re_{13}(\Re_1 + \Re_{g1} + \Re_2)}{\Re_{11} + \Re_1 + \Re_{g1} + \Re_2 + \Re_{13}} \quad \Re_{eq1} = \Re_{11} + (\Re_{22} \| \Re_{23})$$

$$\Re_{eq2} = \Re_{22} + (\Re_{11} \| \Re_{23})$$

References

[1] M. Bauer, P. Becker and Q. Zheng, Proc. MAGLEV (2006).
[2] G. Nissen, Proc. MAGLEV (2008).
[3] M. Chen, D. Xu, D. Zhou, and X. Wu, Proc. APEC 1165 (2004).
[4] A. P. Hu, PhD Thesis, University of Auckland, New Zealand (2001).
[5] J. Meins, G. Bühler, R. Czainski, and F. Turki, Proc. MAGLEV (2006).
[6] K.Woo, H. S. Park, Y. H. Cho, and K. H. Kim, IEEE Trans. Magn. **41**, 1596 (2005).
[7] A. J. Moradewicz and M. P. Kazmierkowski, IEEE Trans. Ind. Electron. **57**, 3181 (2010).
[8] C. Kim, D. Seo, J. You, J. Park, and B. H. Cho, IEEE Trans. Ind. Electron. **48**, 1238 (2001).
[9] J. Sallan, J. L. Villa, A. Llombart, and J. F. Sanz, IEEE Trans. Ind. Electron. **56**, 2140 (2009).
[10] C. Wang, O. H. Stielau, and G. A. Covic, IEEE Trans. Ind. Electron. **52**, 1308 (2005).
[11] X. Liu, W. M. Ng, C. K. Lee, and S. Y. Hui, Proc. APEC 645 (2008).